SUPLEMENTAL INFORMATION

Spontaneous ligand loss by soft-landed $[Ni(bpy)_3]^{2+}$ ions on perfluorinated self-assembled monolayer surfaces

Hugo Y. Samayoa-Oviedo,[1] Harald Knorke,[2] Jonas Warneke,[*,2,3] and Julia Laskin[*,1]

[1]*Department of Chemistry, Purdue University, West Lafayette, IN 47907, United States*

[2] *Wilhelm-Ostwald-Institut für Physikalische und Theoretische Chemie, Universität Leipzig, 04103 Leipzig, Germany.*

[3]*Leibniz Institute of Surface Engineering (IOM), Sensoric Surfaces and Functional Interfaces, Permoserstr. 15, D-04318 Leipzig, Germany.*

*Corresponding authors:

Julia Laskin, Tel: 765-494-5464, Email: jlaskin@purdue.edu

Jonas Warneke, Email: Jonas.warneke@uni-leipzig.de

Table of Contents:

Table S3. Calculated angles between two bpy of $[Ni(bpy)_3]^{2+}$, $[Ni(bpy)_2]^{2+}$ and $[B_{12}F_{12}]^{2-}[Ni(bpy)_3]^{2+}$ in the gas phase and in the presence of the model surface $C_{54}H_{72}$.

Figure S8. Visualization of the angle between the planes spanned by two bpy molecules for $[Ni(bpy)_2]^{2+}$ singlet and $[Ni(bpy)_3]^{2+}$ triplet.

Link to database containing the calculated structures.

Table S1. Instrumental settings for the deposition of $[Ni(bpy)_3]^{2+}$.

Element	Value
ESI voltage	3500 V
Inlet	390 V
Repeler in	460 V
Repeler out	280 V
HPF in	300 V
HPF out	100 V
HPF frequency	675 kHz
RF_{p-p} HPF	134 V
Pressure	8.0 torr
LPF in	88 V
LPF lens	36 V
LPF out	33 V
LPF frequency	890 kHz
RF_{p-p} LPF	85 V
Pressure	1.0 torr
CC bias	29.1 V
CC lens	27.9 V
CC frequency	1.805 MHz
RF_{p-p} CC	703 V
Pressure	3.9×10^{-2} torr
Bent ion guide bias	18.4 V
Bent ion guide frequency	1.732 MHz
RF_{p-p} BF	230 V
Pressure	1.8×10^{-4} torr
TK lens 1	9 V
TK lens 2	-40 V
Pre-filter	23.1 V
Resolving quadrupole frequency	555 kHz
Mass analyzer bias	-3.9 V
Post-filter	23 V
Exit	6 V
Einzel 1 and 3	-50 V
Einzel 2	15 V
Metal plate (mask)	5 V
Surface bias	22 V
Pressure	4.8×10^{-6} torr

Table S2. Measured and expected *m/z* values of species observed on surfaces shown in this work.

Label	Assignment	Measured *m/z*	Expected *m/z*	Mass difference [mDa]
1	$[Ni(bpy)_3]^{2+}$	263.0708	263.0703	0.5
1.a	$[Ni(bpy)_2(bpyD)]^{2+}$	267.0951	267.0954	-0.3
1.b	$[Ni(bpy)(bpyD)_2]^{2+}$	271.1202	271.1205	-0.3
1.c	$[Ni(bpyD)_3]^{2+}$	275.1451	275.1456	-0.5
2	$[Ni(bpy)_2]^{2+}$	185.0363	185.0359	0.4
2.a	$[Ni(bpy)(bpyD)]^{2+}$	189.0606	189.0610	-0.4
2.b	$[Ni(bpyD)_2]^{2+}$	193.0860	193.0861	-0.1
3	$[Ni(bpy)]^{2+}$	107.0024	107.0015	0.9
4	$[Ni(bpy)_2Cl]^{+}$	404.9883	405.0411	-2.8
5	$[Ni(bpy)_2(C_{16}H_{31}O_2)]^{+}$	625.3037	625.3047	-1.0
6	$[Ni(bpy)_2(C_{18}H_{35}O_2)]^{+}$	653.3290	653.3360	-7.0
7	$[Ni]^{+}$	57.9352	57.9348	0.4
8	$[Ni(bpy)(CH_3CN)]^{2+}$	127.5150	127.5148	0.2
9	$[Ni(bpy)]^{+}$	214.0029	214.0035	-0.6
10	$[Ni(bpy)(OH)]^{+}$	231.0068	231.0063	0.5
11	$[Ni(bpy)(Cl)]^{+}$	248.9722	248.9724	-0.2
12	$[Ni(bpy)(C_3H_5O_3)]^{+}$	303.0274	303.0274	0.0
13	$[Ni(bpy)(C_{14}H_{27}O_2)]^{+}$	441.2031	441.2047	-1.6
14	$[Ni(bpy)(C_{15}H_{29}O_2)]^{+}$	455.2183	455.2203	-2.0
15	$[Ni(bpy)(C_{16}H_{31}O_2)]^{+}$	469.2340	469.2360	-2.0
16	$[Ni(bpy)(C_{18}H_{35}O_2)]^{+}$	497.2637	497.2673	-3.6
17	$[Ni(bpy)_2(CH_3CN)_2]^{2+}$	226.0595	226.0624	-2.9
18	$[Ni(bpy)_2(CH_3CN)_3]^{2+}$	246.5728	246.5757	-2.9
19	$[Ni(bpy)_2(C_3H_5O_2)]^{+}$	443.0981	443.1012	-3.1
20	$[Ni(bpy)_2(C_6H_{11}O_2)]^{+}$	485.1443	485.1482	-3.9
21	$[Ni(bpy)_2(C_9H_{17}O_2)]^{+}$	527.1915	527.1952	-3.7
22	$[Ni(bpy)_3(C_2H_6)]^{+}$	556.1825	556.1880	-5.5
23	$[Ni(bpy)_2(C_{14}H_{27}O_2)]^{+}$	597.2694	597.2734	-4.0
24	$[Ni(bpy)_2(C_{15}H_{29}O_2)]^{+}$	611.2840	611.2890	-5.0
i	$[bpy]^{+}$	156.0684	156.0682	0.2
ii	$C_9H_{19}N_2^{+}$	155.1547	155.1548	-0.1

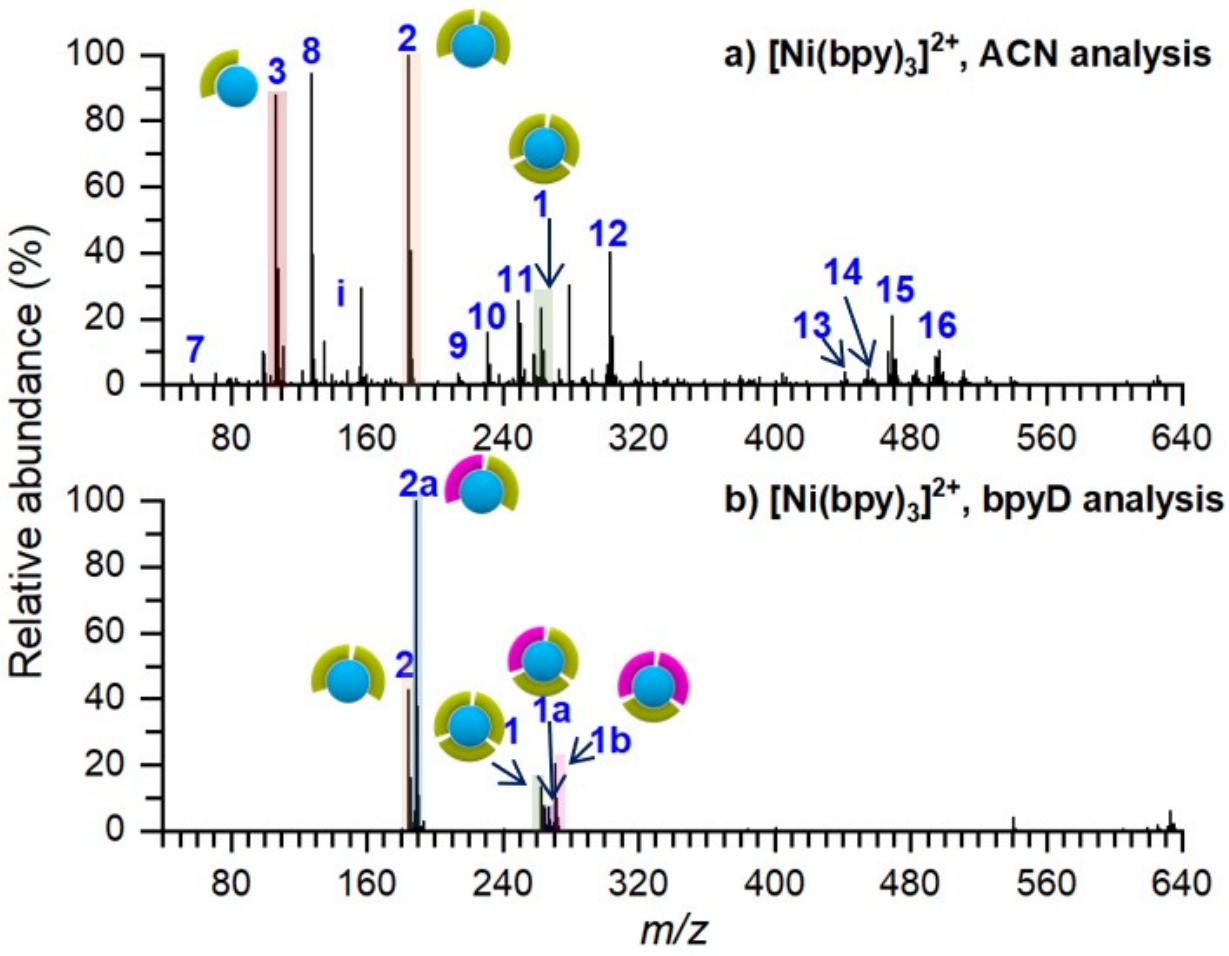

Figure S1. *Ex-situ* nano-DESI MS over a wider *m/z* range of the deposition spots of $[Ni(bpy)_3]^{2+}$ analyzed with a) ACN and b) 3 μM bpyD in ACN as the nano-DESI solvent. Ion assignments are listed in Table S2.

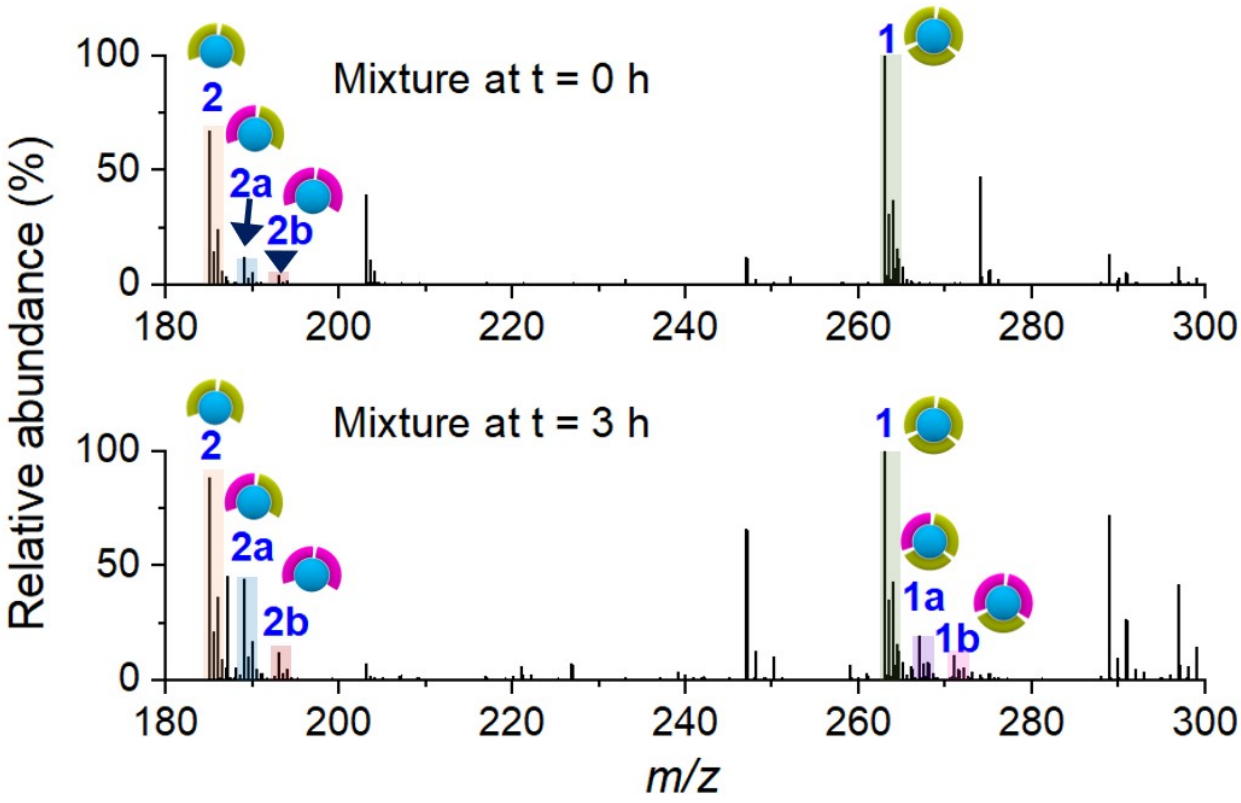

Figure S2. Mass spectrum of a solution containing 15 µM $Ni(bpy)_3SO_4$ and 15 µM bpyD measured right after preparing the solution (top) and after 3 hours of preparing the solution (bottom).

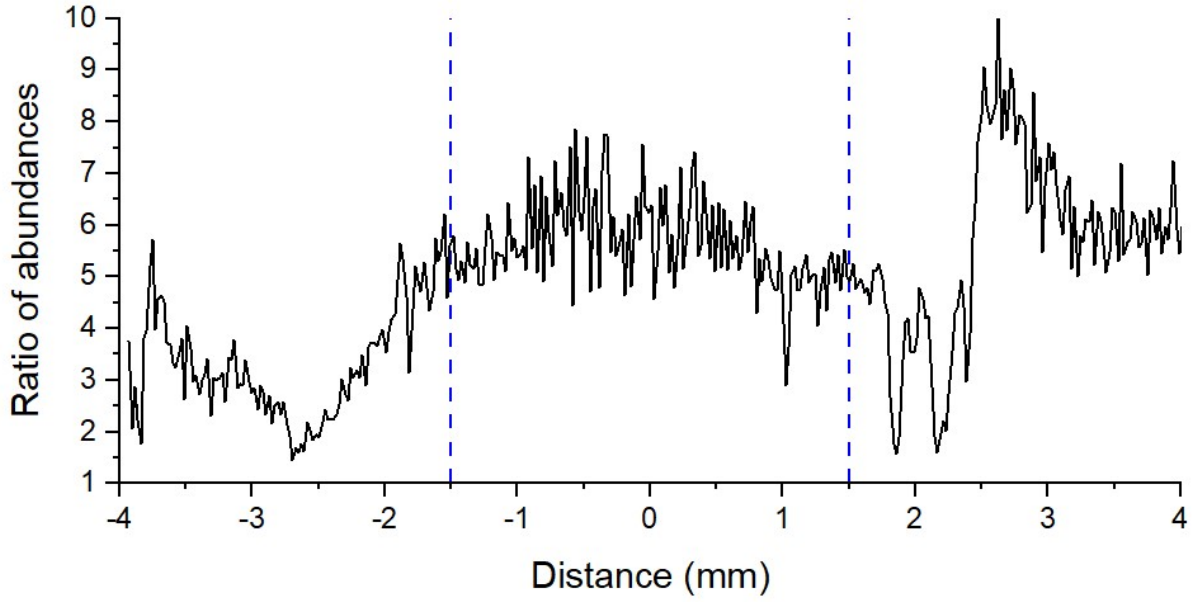

Figure S3. Abundance ratio of $[Ni(bpy)_2]^{2+}/[Ni(bpy)_3]^{2+}$ across the deposition spot for the deposition of $[Ni(bpy)_3]^{2+}$.

The figure above shows the ratio of abundances of $[Ni(bpy)_2]^{2+}/[Ni(bpy)_3]^{2+}$. We observe that $[Ni(bpy)_2]^{2+}$ is higher in abundance in the center of the deposition spot (between -2 and 2 mm) with respect to $[Ni(bpy)_3]^{2+}$. The $[Ni(bpy)_2]^{2+}/[Ni(bpy)_3]^{2+}$ ratio increases from ~2 on the periphery of the deposition spot (-2.5 mm) to ~6 in the center of the spot. The change in the ratio in the 2.5-4 mm region is attributed to the differences in the "carryover" effect due to the analytes having high ionization efficiency and being "sticky" on the capillary. Meanwhile, the ratios observed at positions from -4 mm to -2.5 mm are uncertain due to the low signals of the two ions in this region. This analysis shows that there is a noticeable difference between the traces shown in **Figures 4c** and **4d** beyond the experimental error.

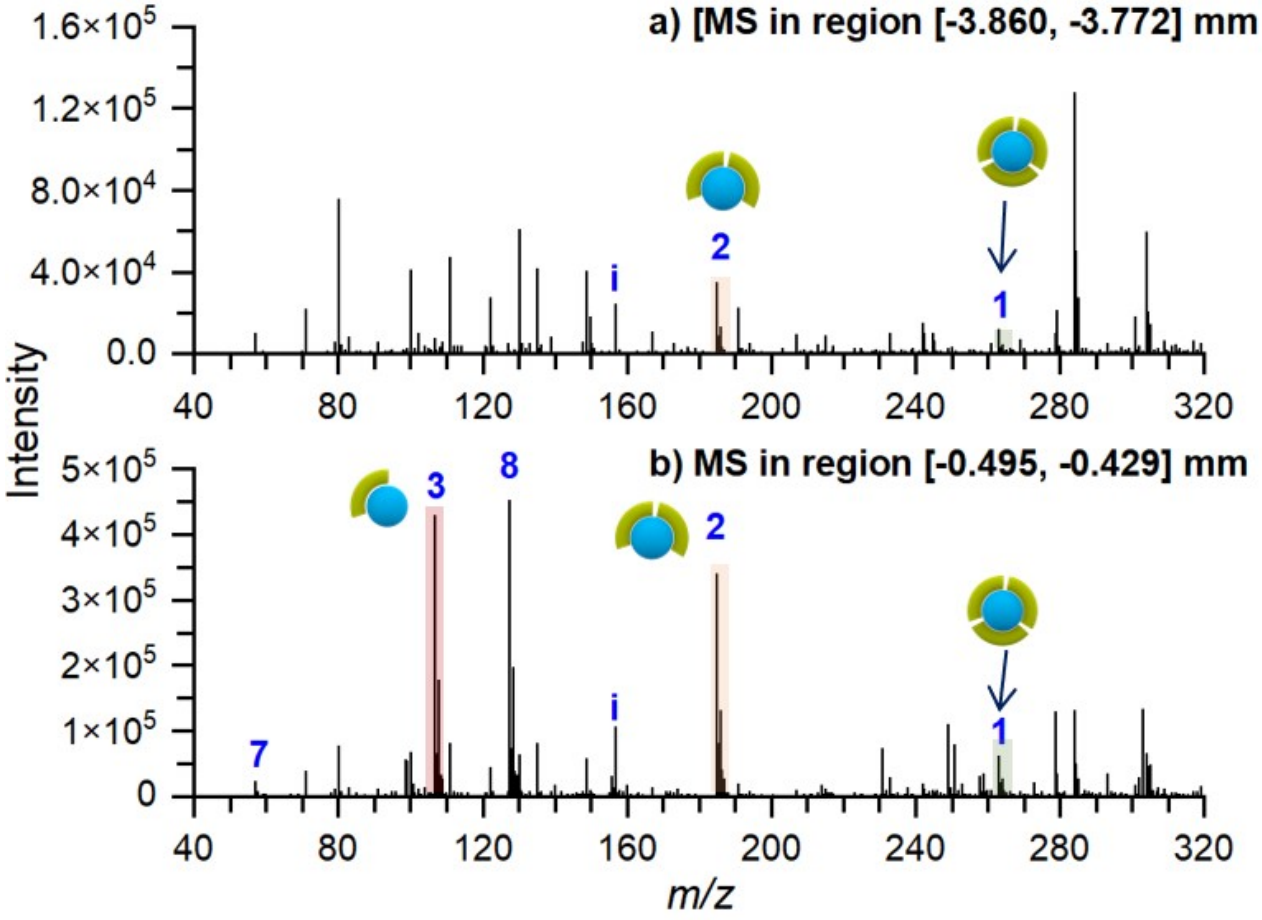

Figure S4. Mass spectra of the surface where $[Ni(bpy)_3]^{2+}$ was deposited on two different regions of the deposition area. The top mass spectrum was acquired by averaging the ion signal in the region at the edges of the deposition spot and the bottom mass spectrum was acquired by averaging the ion signal in the region at the center of the deposition spot.

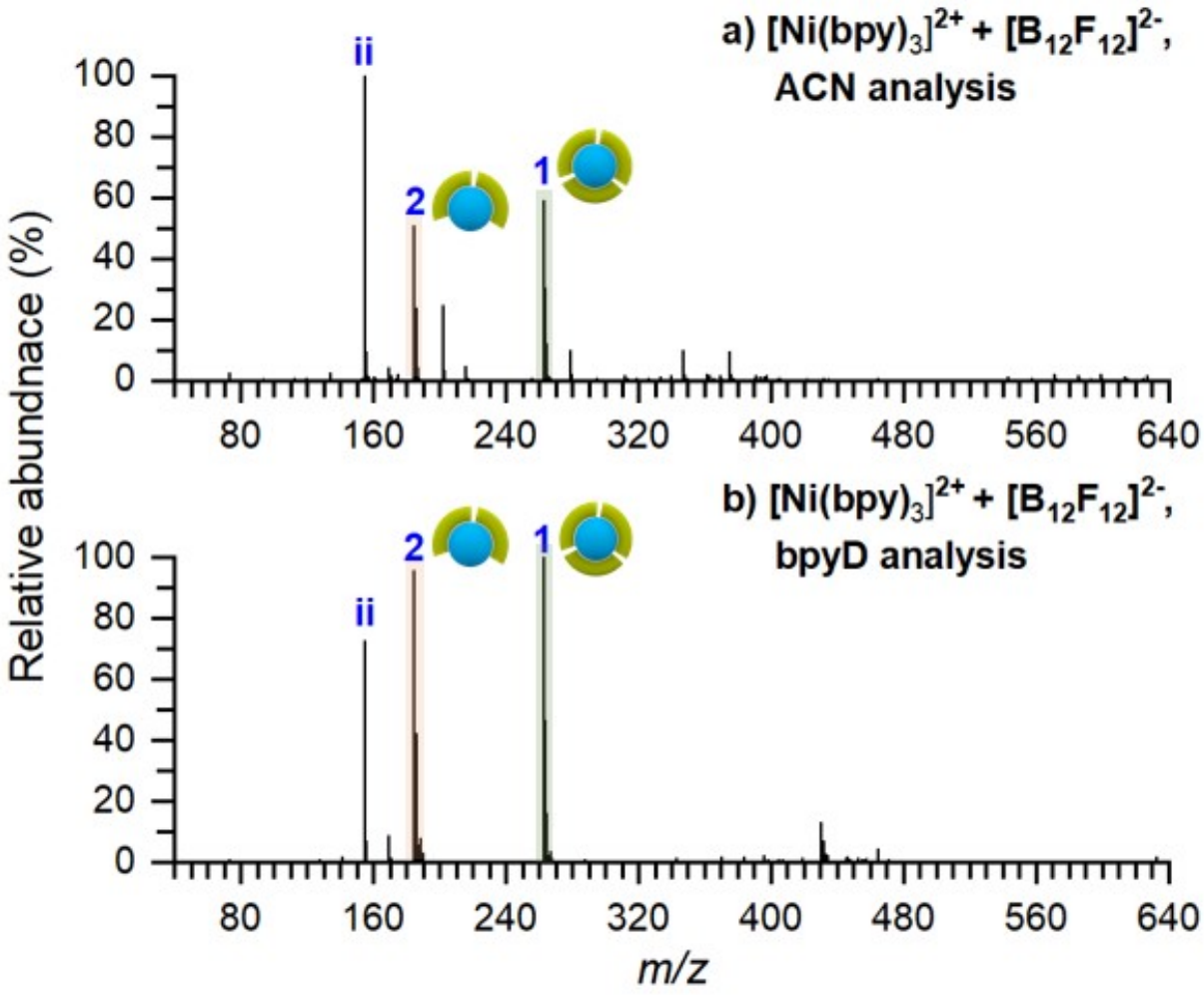

Figure S5. *Ex-situ* mass spectrum of the surface prepared by codeposition of $[Ni(bpy)_3]^{2+}$ and $[B_{12}F_{12}]^{2-}$ analyzed with a) ACN and b) 3 μM bpyD in ACN as the nano-DESI solvent. Ion assignments are listed in Table S2.

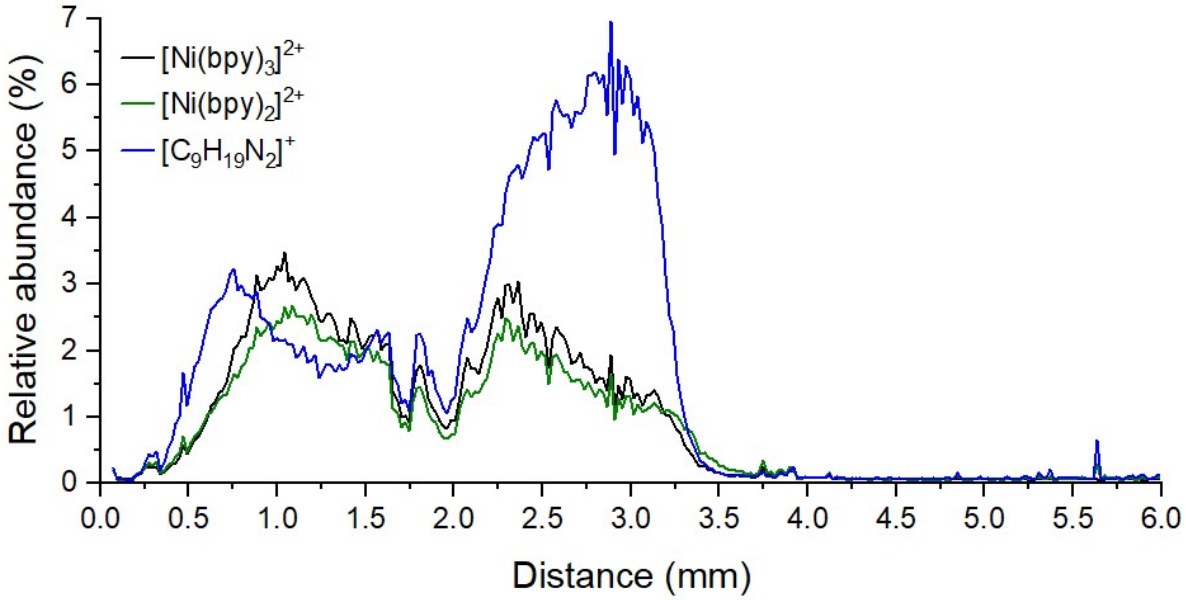

Figure S6. Line scans of the mass spectra in **Figure 6a**. It seems that $[C_9H_{19}N_2]^+$ (**ii**) is colocalized with the Ni-containing species.

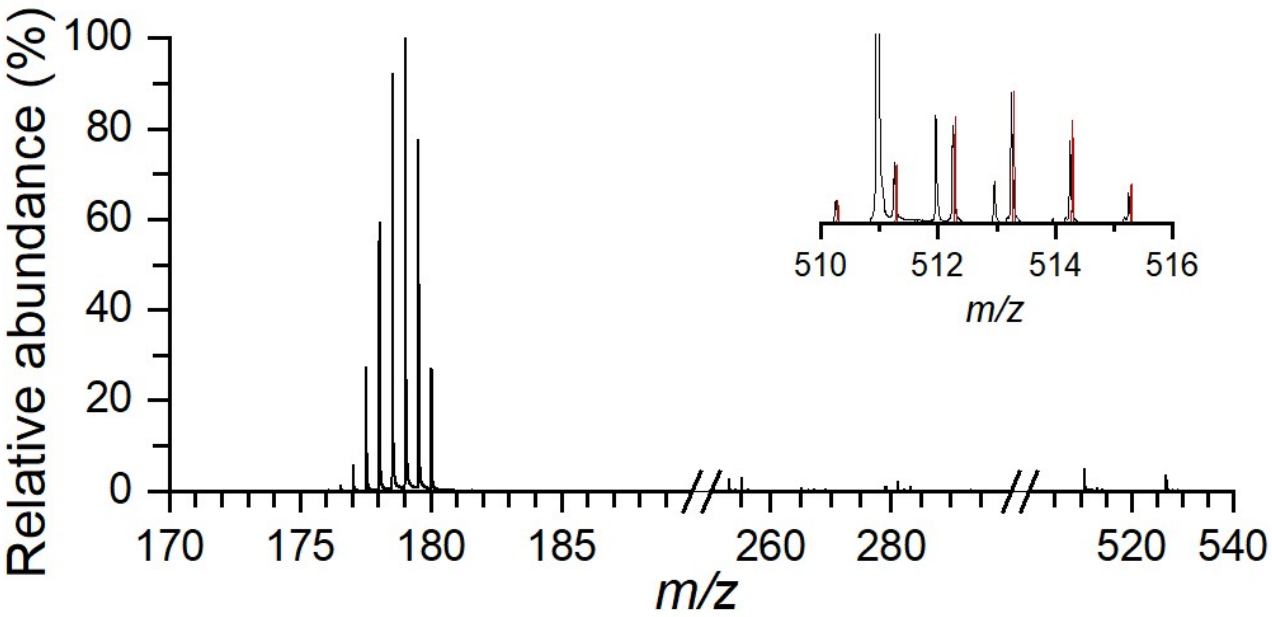

Figure S7. *Ex-situ* mass spectrum in negative mode of the surface prepared by codeposition of $[Ni(bpy)_3]^{2+}$ and $[B_{12}F_{12}]^{2-}$ analyzed with ACN as the nano-DESI solvent. The ion at 179.04954 *m/z* is $[B_{12}F_{12}]^{2-}$. The inset shows a 100x zoom into the 510-516 *m/z* range. The red traces are the isotopic distribution of $[(B_{12}F_{12})(C_9H_{19}N_2)]^-$ overlaying with the experimental trace in black.

Table S3. Calculated angles between two bpy of $[Ni(bpy)_3]^{2+}$, $[Ni(bpy)_2]^{2+}$ and $[B_{12}F_{12}]^{2-}[Ni(bpy)_3]^{2+}$ in the gas phase and in the presence of the model surface $C_{54}H_{72}$. Shown in brackets are the angles between two bpy-ligands where one bpy is not in contact with the surface. The angle between two bpy is determined by the angle between the two planes spanned by the Ni and the two N of each bpy. An example of these angles is shown in Figure S6. Values are calculated at B3LYP+GD3BJ def2SVPP level of theory.

System	Angle in gas phase	Angle on surface	NPA charge of Ni-bpy on surface
$[Ni(bpy)_3]^{2+}$ triplet	3 × 88.9°	80.1° (86.4°, 89.6°)	1.99 *e*
$[B_{12}F_{12}]^{2-}$ $[Ni(bpy)_3]^{2+}$ triplet	3 × 87.1°	89.1° (87.7°, 84,8°)	−1.84 *e*, 1.88 *e*
$[Ni(bpy)_2]^{2+}$ triplet	46.3°	n. a.	n. a.
$[Ni(bpy)_2]^{2+}$ singlet	36.4°	27.8°	1.98 *e*

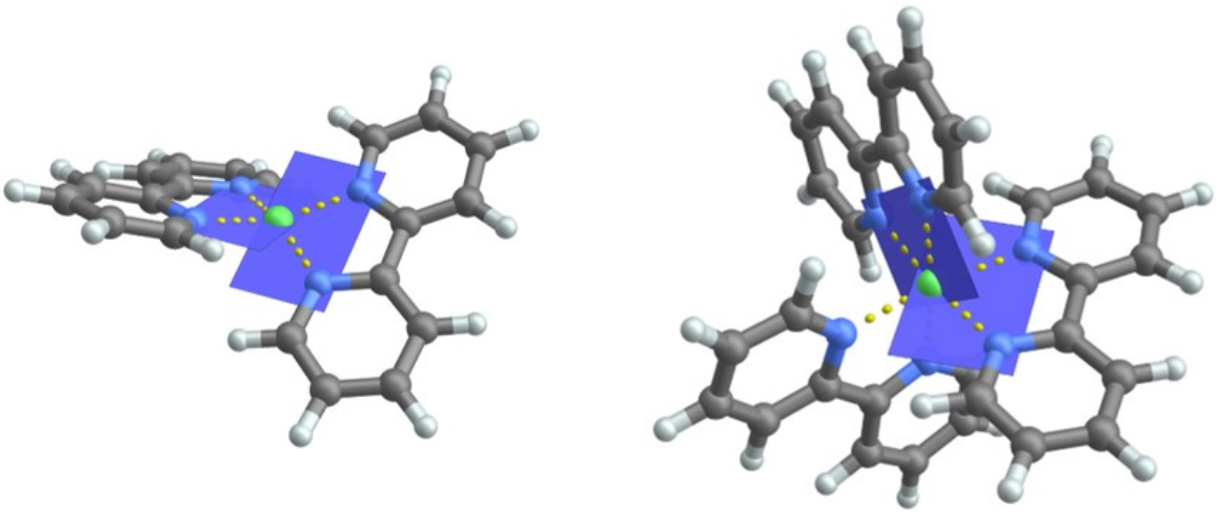

Figure S8. Visualization of the angle between the planes spanned by two bpy molecules for $[Ni(bpy)_2]^{2+}$ singlet and $[Ni(bpy)_3]^{2+}$ triplet.

Link to database containing the calculated structures.

https://nam04.safelinks.protection.outlook.com/?url=https%3A%2F%2Fiochem-bd.bsc.es%2Fbrowse%2Fhandle%2F100%2F320023&data=05%7C02%7Chsamayoa%40purdue.edu%7Cef0f85dbd4444adc332b08dc5e220222%7C4130bd397c53419cb1e58758d6d63f21%7C0%7C0%7C638488747412592813%7CUnknown%7CTWFpbGZsb3d8eyJWIjoiMC4wLjAwMDAiLCJQIjoiV2luMzIiLCJBTiI6Ik1haWwiLCJXVCI6Mn0%3D%7C0%7C%7C%7C&sdata=KGokYMoq9eSVwmoZdMRoQgO8tttY5WTbwkW72oeUlw4%3D&reserved=0